Communications

DOI: 10.1002/anie.200501711

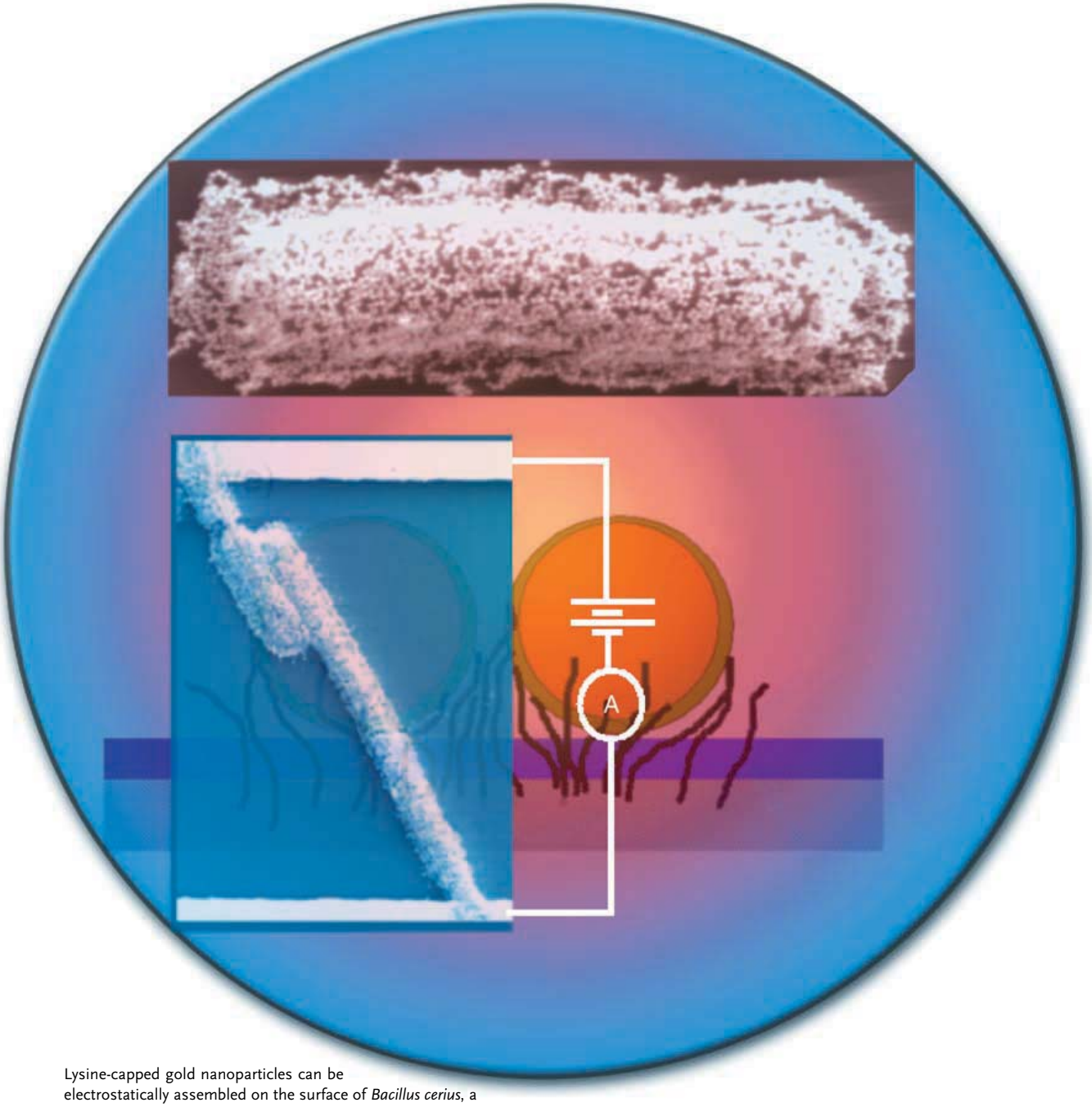

Lysine-capped gold nanoparticles can be electrostatically assembled on the surface of *Bacillus cerius*, a Gram-Positive bacterium. The conductivity of the "gold-plated" bacteria assembly immobilized between electrodes is a function of the humidity experienced by the nanoparticles. For more details on this bioelectronic device, see the Communication by R. F. Saraf and V. Berry on the following pages.

Nanodevices

DOI: 10.1002/anie.200501711

Self-Assembly of Nanoparticles on Live Bacterium: An Avenue to Fabricate Electronic Devices**

*Vikas Berry and Ravi F. Saraf**

Recently, hybrid structures of microorganisms with inorganic nanoscale moieties have received great interest owing to their potential in fabricating electronic systems. The electronic properties of metal nanoparticles, as a result of the single-electron transport of current,[1] make them ideal materials for nanodevices. Concomitantly, the nanostructure of microorganisms such as bacteria,[2] viruses,[3,4] and yeast[5] are attractive scaffolds for the templating of metal nanoparticles through the interactions of the former with surface charges and the affinity of certain metals for specific biological molecules.[2–7] However, the key challenges in building hybrid devices are 1) to pattern nanostructures without destroying the biological construct of the microorganism and 2) to achieve active integration of a biological response to the electrical transport in a nanoparticle device.

Herein, we present a simple method to build hybrid devices that use the biological response of a microorganism to control the electrical properties of the system. In our design, a monolayer of gold nanoparticles is deposited on the peptidoglycan membrane of a live Gram-positive bacterium. The hydrophilic peptidoglycan membrane is then actuated by humidity to modulate the width of the electron-tunneling barrier between the metal nanoparticles. A decrease in interparticle separation by less than 0.2 nm (decrease in humidity from 20 to $\approx 0\,\%$) causes more than a 40-fold increase in tunneling current. Vapor sensors based on the increase in resistance due to separation of Au nanoparticles have been reported in three-dimensional (3D) clusters of Au nanoparticle/organic composite films.[8–10] In the present study, the coupling between the large expansion of an underlying hygroscopic bacterium membrane and the monolayer of Au particles is key to achieving a larger change in current, by an order of magnitude, relative to the above-mentioned 3D nanocomposite devices, for which the change in current results from the swelling of an interparticle organic phase. The method shown herein could be used to pattern various nanoscale inorganic materials, whose optical, electrical, and magnetic properties could be biologically controlled, and thereby lead to an important advance in the present technology.

Electrically percolating clusters of metal nanoparticles, in contrast to their microparticle cousins, are fundamentally different in terms of electrical properties as a result of the nature of interparticle electron transport.[1] On the nanoscale, the energy cost to insert a single electron in a nanoparticle is over 1–10 times greater than the thermal energy, and the flow of the interparticle current takes place through the transport of single electrons, as explicitly shown by transport studies on single nanoparticles,[11,12] their 2D and 3D assemblies,[13–16] and single-nanoparticle devices (such as single-electron transistors[17,18]). The above studies demonstrate that a percolating cluster of metal nanoparticles is a viable unit to fabricate single-electron devices, whereby micron-scale clusters allow an easy-to-fabricate, robust interconnection network for the nanodevice system. Because metal nanoparticles such as gold are stabilized in solution by electrostatic repulsion, the formation of a percolating cluster on physical substrates requires either an organic cross-linker to bind the particles[13,19] or a polyelectrolyte to shield the charge of the particles.[16,20] For biological substrates, the highly selective deposition of nanoparticles relies on either highly specific binding (such as DNA hybridization[21–23] or biotin–streptavidin interactions[24]) or strong specific intermolecular interaction (such as electrostatic interactions[25–27]).

Bacillus cereus, a Gram-positive bacterium, was deposited by using a previously described technique on a silicon substrate with a layer of 500 nm of thermally grown silica and gold electrode lines spaced 7 ± 0.2 microns apart and coated with poly(L-lysine) (average molecular weight 164 kDa).[2] In a typical deposition process, the bacteria were cultured in nutrient broth (Difco) in a shake flask for approximately 14 h at 30 °C. The bacteria were subsequently filtered and centrifuged to extract similar sized cells that were around 4–6 μm in length and 0.8–1.0 μm in diameter. The bacteria were suspended again in sterile water and were deposited on the poly(L-lysine)-coated substrate. On the substrate, there are 20 sets of electrodes. The deposition time of the bacteria was approximately 10–15 min to form bridges spanning the Au electrodes. Usually, about 10 bridges were formed along the 10-mm-long Au electrode pair. The extracellular polymeric substances (EPS) on the bacteria (and around the bacterium) were removed by washing with 2 N NaOH for 1 min. The bacteria-deposited chip was then immediately immersed in a solution of poly(L-lysine)-coated gold nanoparticles (of diameter $d = 30$ nm).[2] Highly controlled deposition of nanoparticles was achieved by regulating the deposition time in the solution of gold nanoparticles (see Figure 1 a–e). As the Au nanoparticles and the substrate are both positively charged, the deposition is highly selective with formation of the monolayer only on the negatively charged bacteria surface. However, a simple negative surface charge is not sufficient to obtain electrically percolating deposition. Figure 1 f shows the result of deposition of Au nanoparticles on a negatively charged physical surface prepared by

[*] V. Berry, Prof. R. F. Saraf
Department of Chemical Engineering
University of Nebraska
Lincoln, NE 68588 (USA)
Fax: (+1) 402-472-6989
E-mail: rsaraf@unlnotes.unl.edu

[**] R.F.S. thanks the Optical Science and Engineering Research Center, Virginia Tech, and the ONR for financial support. We thank Dr. Inan at the University of Nebraska for his help in identifying the assay to determine the fate of the bacteria at various stages of the device fabrication. We thank Dr. Adenwalla at the University of Nebraska for allowing us access to a low-temperature *I–V* measurement system.

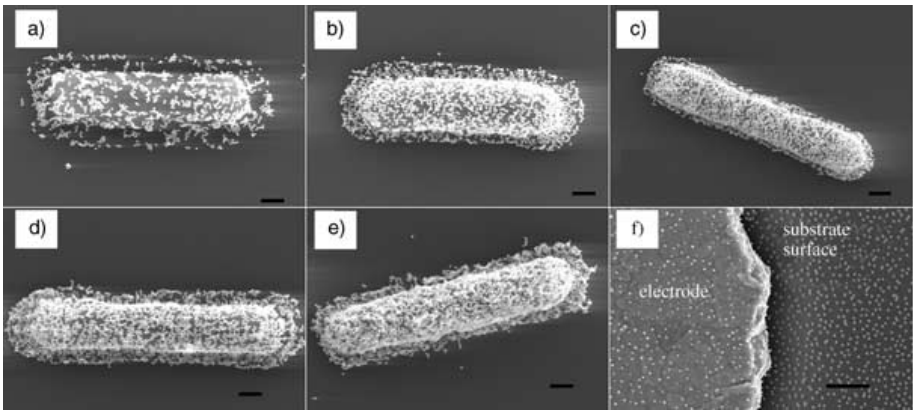

Figure 1. Scanning electron microscopy (SEM) images reveal the highly controlled and selective deposition on bacteria of poly(L-lysine)-coated 30-nm Au nanoparticles from a solution at pH 7 over a) 30 min, b) 1 h, c) 2 h, d) 4 h, and e) 8 h. f) Positively charged Au nanoparticles are deposited on a negatively charged PSS-coated lysine/SiO_2/Si substrate over 16 h. The Au nanoparticles percolate after deposition during 4 h on the bacteria, while no conduction is observed for the physical surface in (f). The small amount of multilayer formation with a long deposition time is due to contraction of the membrane through loss of water in the scanning electron microscope. Scale bar: 300 nm.

adsorbing a monolayer of poly(sulfonated styrene) (PSS; 70 kDa with $<90\,\%$ sulfonation) on the poly(L-lysine)-coated SiO_2/Si substrate. For maximal deposition, poly(L-lysine) and PSS were introduced at pH values of around 4 and 8.5, respectively, and 1 mM NaCl was added to the suspension of the nanoparticles at pH 7. However, the 2D packing density was found to be low and nonpercolating. X-ray reflectivity measurements showed that in the multilayer films of polyelectrolytes (in our case, PSS on poly(L-lysine)) the polymers are layered and their conformations are flat with no significant loops caused by multiple-point binding.[28] As a result, the mobility of the polymer is highly restricted. On the other hand, the polyelectrolyte on the bacterium surface, that is, teichoic acid (-$OCH_2CH(OCH_3)CH_2OPO_2$-), is a flexible "brush" that is tethered to the peptidoglycan surface at one end which leaves the remainder of the chain in high thermal motion (i.e. high mobility). Furthermore, because the brush contour length is typically around 18 nm,[29] it is reasonable to expect that the negatively charged teichoic acid molecule with its high mobility and chain flexibility may wrap over the positively charged Au nanoparticle up to a maximum possible subtended angle of 135° from the point of contact to minimize the free energy. A similar screening of charge by PSS would be difficult in the case of the PSS–poly(L-lysine) structure owing to restricted mobility. Specific attachment of a concanavalin–fluorescein isothiocyanate dye conjugate to teichoic acid[30] followed by confocal microscopy confirmed the uniform distribution of the acid molecules on the bacterium. As no deposition of nanoparticles on the bacterium occurs subsequent to the neutralization of teichoic acid after attachment with concanavalin, the role of the acid in high-density deposition is justified.

A standard assay of PI/SYTO 9 dye was used to confirm the fate of the bacteria.[31] The green fluorescence in Figure 2 confirms that the bacteria survived the complete fabrication process of the device. As the integrity of the peptidoglycan surface membrane in which the teichoic acid molecular brush is imbedded is critical for the deposition of Au nanoparticles, the survival of the bacteria for the fabrication of the device is important: Any lysis of the bacteria (or release of EPS and/or internal bacterial fluids) will lead to ill-formed, nonfunctional devices.

The insets of Figure 3 show a typical bacterial bridge, coated with a monolayer of gold nanoparticles, con-

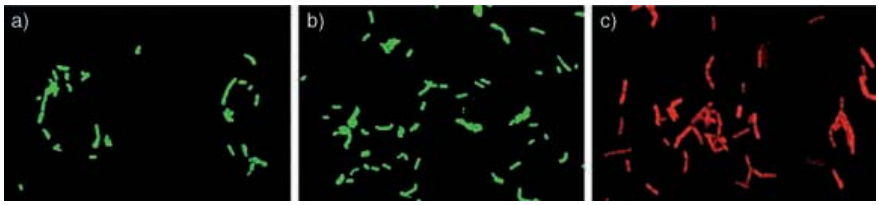

Figure 2. The standard PI/SYTO 9 assay in combination with confocal microscopy is used to probe the survival of the bacteria at various stages of the fabrication process: a) immediately after immobilization from the nutrient broth on the substrate; b) after deposition of the gold nanoparticles over 4 h; and c) after subjecting to 10^{-5} Torr vacuum for 2 h. The green and red fluorescence indicate that the bacteria are alive and dead, respectively.

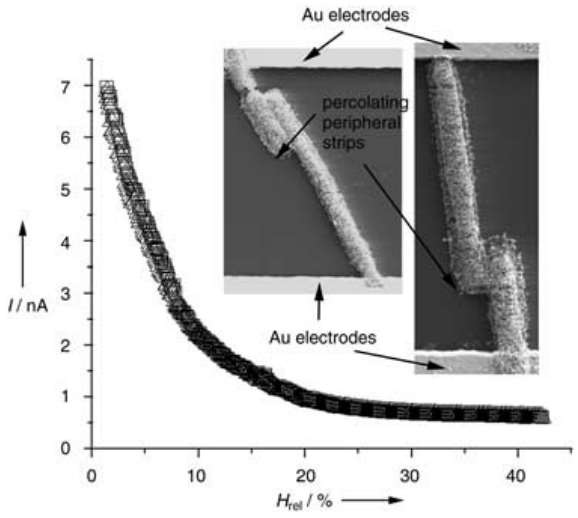

Figure 3. Typical device current (I, normalized per bridge) as a function of relative humidity (H_{rel}) for "up" (i.e. decreasing humidity; △) and "down" cycles (i.e. increasing humidity; □) at a bias voltage of 10 V. The inset shows SEM images of two typical bacteria bridges which span the electrodes. The peripheral strip is a (percolating) monolayer of deposited gold nanoparticles.

nected to the gold electrodes. One bridge constitutes a device. All the currents reported subsequently were measured at 22 °C and were normalized according to the number of bridges between the electrodes. Figure 3 depicts the normalized current, I, between the bridges as a function of the relative humidity, H_{rel}. The deposition of the Au nanoparticles was optimized for 4 h (see Figure 1) to obtain the largest change in current due to humidity. Figure 3 indicates that the device behavior is reversible and stable over a slow run, measured over approximately 40 min per cycle. Because of the complete reversibility of the device, it is unlikely that the water inside the bacteria plays any significant role. In contrast to most impedance-based microelectronic humidity probes,[32] the resistance of this device decreases as humidity increases. The largest change in current, and hence the highest sensitivity, was observed for the low humidity region of $H_{rel} < 20\,\%$.

The simple model shown in Figure 4 explains the observation in Figure 3. As the humidity increases, the peptidoglycan membrane absorbs water. If it is assumed that there is no

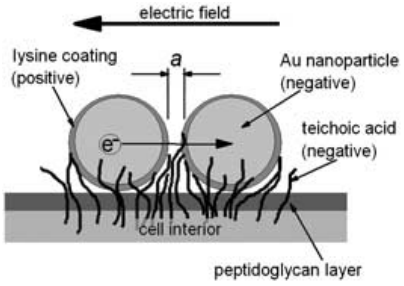

Figure 4. Schematic showing two poly(L-lysine)-coated Au nanoparticles clutched by negatively charged teichoic acid molecules. The distance between the surfaces of the Au nanoparticles is given by *a*. The electron transport from left to right takes place across a mixture of organics (lysine, teichoic acid) and air. The role of the electric-field-inducing electron transport is discussed in Figures 3 and 5.

excess volume of absorbed water, the volume fraction of water absorbed is fH_{rel}, in which f is Henry's constant. If it is also assumed that there is affine swelling of the peptidoglycan membrane, the linear extension of the membrane due to absorption is $(1-fH_{rel})^{-1/3}$. As the nanoparticles are fixed on the membrane, the interparticle separation is given by $a/a_0 = (1-fH_{rel})^{-1/3}$, where a_0 is the separation at $H_{rel} = 0$. Also, as electron tunneling is the primary transport mechanism, the current is given by the Fowler–Nordheim equation [Eq. (1)],[33] where $K = (32\pi^2 m_e \varphi/h^2)^{0.5}$ (h is Planck's constant, m_e is the mass of an electron at rest, and φ is the barrier height at the nanoparticle/organic interface), R_B is the resistance to the leakage current from the peripheral as shown in Figure 3, R_0 is a normalization constant proportional to the resistance of the device at $H_{rel} = 0$, and V is the bias across the device (i.e. the bacteria bridge).

$$I = \left\{ \frac{V}{R_0} \exp\left[-\frac{K a_0}{\sqrt[3]{(1-f H_{rel})}} \right] + \frac{V}{R_B} \right\} \qquad (1)$$

We assume that the peripheral strip that leads to finite R_B is due to deposition of proteinaceous substances secreted by the bacterium (probably for adhesion to the substrate). To study the effect of water absorption by poly(L-lysine) on the performance of the device after the fabrication of the device, we capped the amine groups of poly(L-lysine) with glutaraldehyde to decrease the water uptake by lysine. No significant change in the performance of the device was observed which indicates that the role of moisture absorption by poly(L-lysine) on the performance is negligible.

Figure 5a shows the fit of the experimental results to Equation (1) for the same device at different bias V. Each exposure to humidity lasted approximately 40 min, and the lapse between consecutive runs was about 1 h on average. Although Equation (1) requires four fitting parameters, the validity of the model is justified because they are reasonably constant over all the biasing voltages (see Figure 5b). The constant R_B implies ohmic behavior (independent of H_{rel}) for leakage current given by $I_B = V/R_B$. This is reasonable because on the peripheral region, the nanoparticles are not located on the peptidoglycan membrane but adsorbed onto proteinaceous corona of the bacteria that do not change significantly in the lateral dimension with humidity. As the contact resistance is not expected to be large[2] and is a strong function of humidity, it is included in R_B. We also note that because the current through a bacteria bridge that lacks deposited gold nanoparticles is insignificant, ionic currents can be neglected.

Figure 5c shows the corrected current, $I-I_B$, which flows through the nanoparticle monolayer as a function of the change in the interparticle separation (estimated from f). Interestingly, for a humidity change from 20 to 0 %, which corresponds to a calculated decrease of only 7 % in the interparticle distance, the corrected current increases over 40-fold. As the corresponding increase in the total current I is only about sevenfold (see Figure 5a), a decrease in peripheral deposition will improve the device sensitivity significantly. The high sensitivity to subtle changes in the interparticle distance is attributed to transport by single-electron tunneling through the percolation network because the charging energy $e^2/(2\pi\varepsilon\varepsilon_0 d)$ (ε is the dielectric constant of the organic coating and is approximately 3; e is the electron charge) approximates to $1.5\,kT$. Using the model parameters and a tunneling barrier of 5.1 eV (i.e. a is much larger than the thickness of the coating of poly(L-lysine) shown in Figure 4 at the metal–poly(L-lysine)/air/metal–poly(L-lysine) junction), the nanoparticle separation at 0 % humidity was determined as about 2.3 nm, which implies an absolute change (for the 0–20 % humidity range) of less than 0.2 nm. We note that the sensitivity is significantly lower for devices fabricated with deposition times of greater than 8 h and that ohmic I–V behavior is observed[2] in contrast to the non-ohmic behavior observed for devices prepared with deposition times of 4 h (see Figure 5d). At the other extreme, for a deposition time of 2 h the interparticle distance in the contiguous clusters is too large for a significant tunneling current to be observed. Thus, a combination of the exponential dependence on a and that $a \approx 2.3$ nm explains the high sensitivity of the system. Furthermore, in contrast to the earlier reports on gold nanoparticle/

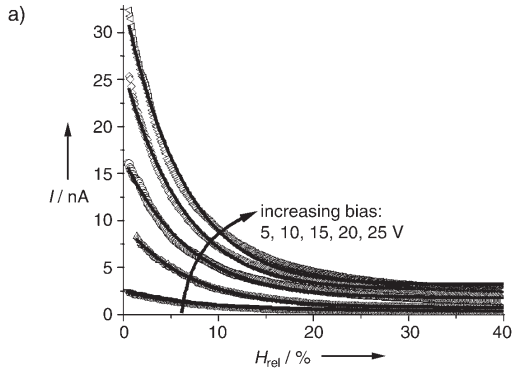

b)

V / V	R_0	K	f	R_B / Ω
5	3.132 E-15	54.97704	0.68127	1.202 E+10
10	3.504 E-15	54.1266	0.7896	1.298 E+10
15	2.888 E-15	54.21572	0.79742	8.311 E+09
20	2.413 E-15	54.22724	0.86098	7.422 E+09
25	2.691 E-15	54.08358	0.86614	7.775 E+09

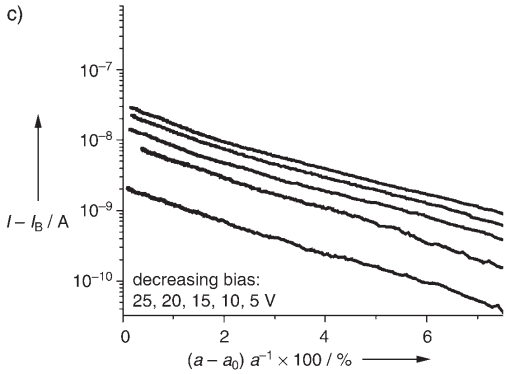

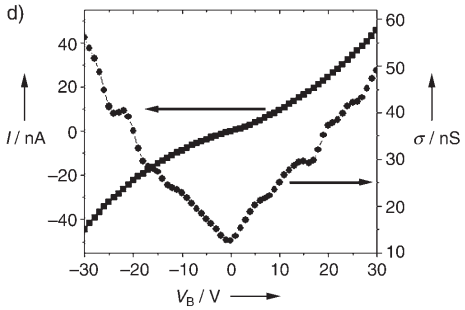

Figure 5. The validity of model and peptidoglycan actuation. a) A comparison of theoretical values (according to Equation (1); solid lines) and experimental observations (data points) for the current I as a function of the relative humidity (H_{rel}) at various bias voltages for the same device. b) The four fitting parameters, K, f, T_0, and R_B. c) The corrected current, $I-I_B$ (after subtraction of the calculated leakage current, I_B) as a function of the calculated percentage change in the interparticle distance, a, due to humidity-induced dimensional changes in the peptidoglycan membrane. Consistent with the model given by [Eq. (1)], the straight line for all bias voltages in the semi log plot indicates an exponential dependence of a. d) The non-ohmic I–V characteristics and differential conductance σ of the device at 2% humidity. ■: current; ●: differential conductance.

organic composite thin-film sensors[8–10] in which electron transport takes place by thermionic emission or activated tunneling, electron transport in our device takes place through tunneling because the activation energy for tunneling is approximately 1.7 meV (see Figure 6), which is much lower than the thermal energy of a free electron ($kT \approx 25$ meV) at room temperature.

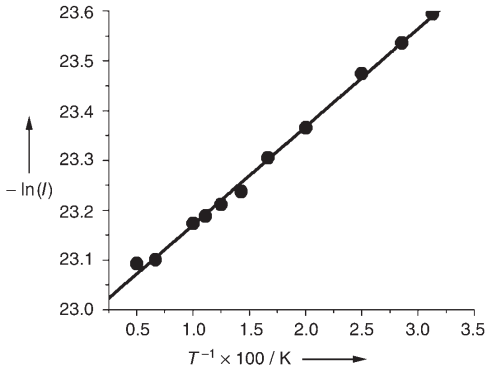

Figure 6. Temperature dependence of the device current at 0% humidity shown by a plot of the negative natural logarithm of the current I at an applied bias of 0.1 V. $I = 1.05 \times 10^{-10} \exp(-\frac{E_a}{kT})$, with an activation energy $E_a = 1.71$ meV.

In summary, we have illustrated an approach to fabricate an active hybrid bioelectronic device using physical nanomaterials and a live microorganism. The electrical properties of a monolayer of gold nanoparticles is controlled by actuating the peptidoglycan layer of the bacterium. An actuation of less than 8% in the peptidoglycan membrane, induced by a change in humidity from 20 to 0%, leads to more than a 40-fold increase in the tunneling current. These results open up an avenue to obtain active coupling between microorganisms and electrical, optical, and/or magnetic nanodevices. We believe that such hybrids will be the key to conceptually new electronic devices that can be integrated with microorganisms on flexible plasticlike substrates by using simple chemistry.

Received: May 18, 2005
Revised: July 27, 2005

Keywords: electrochemistry · gold · monolayers · nanostructures · self-assembly

[1] B. Su, V. J. Goldman, J. E. Cunningham, *Science* **1992**, *255*, 313 – 315.
[2] V. Berry, S. Rangaswamy, R. F. Saraf, *Nano Lett.* **2004**, *4*, 939 – 942.
[3] E. Dujardin, C. Peet, G. Stubbs, J. N. Culver, S. Mann, *Nano Lett.* **2003**, *3*, 413 – 417.
[4] C. E. Fowler, W. Shenton, G. Stubbs, S. Mann, *Adv. Mater.* **2001**, *13*, 1266 – 1269.
[5] M. Kowshik, S. Ashtaputre, S. Kharrazi, W. Vogel, J. Urban, S. K. Kulkarni, K. M. Paknikar, *Nanotechnology* **2003**, *14*, 95 – 100.
[6] Z. Li, S. W. Chung, J. M. Nam, D. S. Ginger, C. A. Mirkin, *Angew. Chem.* **2003**, *115*, 2408 – 2411; *Angew. Chem. Int. Ed.* **2003**, *42*, 2306 – 2309.
[7] N. L. Rosi, C. S. Thaxton, C. A. Mirkin, *Angew. Chem.* **2004**, *116*, 5616 – 5619; *Angew. Chem. Int. Ed.* **2004**, *43*, 5500 – 5503.
[8] N. Krasteva, I. Besnard, B. Guse, R. E. Bauer, K. Mullen, A. Yasuda, T. Vossmeyer, *Nano Lett.* **2002**, *2*, 551 – 555.
[9] H. Wohltjen, A. W. Snow, *Anal. Chem.* **1998**, *70*, 2856 – 2859.
[10] F. P. Zamborini, M. C. Leopold, J. F. Hicks, P. J. Kulesza, M. A. Malik, R. W. Murray, *J. Am. Chem. Soc.* **2002**, *124*, 8958 – 8964.
[11] M. F. Crommie, C. P. Lutz, D. M. Eigler, *Science* **1993**, *262*, 218 – 220.
[12] H. Ohnishi, Y. Kondo, K. Takayanagi, *Nature* **1998**, *395*, 780 – 783.
[13] R. P. Andres, J. D. Bielefeld, J. I. Henderson, D. B. Janes, V. R. Kolagunta, C. P. Kubiak, W. J. Mahoney, R. G. Osifchin, *Science* **1996**, *273*, 1690 – 1693.
[14] H. Imamura, J. Chiba, S. Mitani, K. Takanashi, S. Takahashi, S. Maekawa, H. Fujimori, *Phys. Rev. B* **2000**, *61*, 46 – 49.
[15] A. A. Middleton, N. S. Wingreen, *Phys. Rev. Lett.* **1993**, *71*, 3198 – 3201.
[16] P. E. Trudeau, A. Escorcia, A. A. Dhirani, *J. Chem. Phys.* **2003**, *119*, 5267 – 5273.
[17] T. Sato, H. Ahmed, D. Brown, B. F. G. Johnson, *J. Appl. Phys.* **1997**, *82*, 696 – 701.
[18] C. Thelander, M. H. Magnusson, K. Deppert, L. Samuelson, P. R. Poulsen, J. Nygard, J. Borggreen, *Appl. Phys. Lett.* **2001**, *79*, 2106 – 2108.
[19] M. Brust, D. Bethell, D. J. Schiffrin, C. J. Kiely, *Adv. Mater.* **1995**, *7*, 795.
[20] A. Rosidian, Y. J. Liu, R. O. Claus, *Adv. Mater.* **1998**, *10*, 1087.
[21] E. Braun, Y. Eichen, U. Sivan, G. Ben-Yoseph, *Nature* **1998**, *391*, 775 – 778.
[22] J. D. Le, Y. Pinto, N. C. Seeman, K. Musier-Forsyth, T. A. Taton, R. A. Kiehl, *Nano Lett.* **2004**, *4*, 2343 – 2347.
[23] Y. Maeda, H. Tabata, T. Kawai, *Appl. Phys. Lett.* **2001**, *79*, 1181 – 1183.
[24] H. Y. Li, S. H. Park, J. H. Reif, T. H. LaBean, H. Yan, *J. Am. Chem. Soc.* **2004**, *126*, 418 – 419.
[25] A. Kumar, M. Pattarkine, M. Bhadbhade, A. B. Mandale, K. N. Ganesh, S. S. Datar, C. V. Dharmadhikari, M. Sastry, *Adv. Mater.* **2001**, *13*, 341 – 344.
[26] H. Nakao, H. Shiigi, Y. Yamamoto, S. Tokonami, T. Nagaoka, S. Sugiyama, T. Ohtani, *Nano Lett.* **2003**, *3*, 1391 – 1394.
[27] M. G. Warner, J. E. Hutchison, *Nat. Mater.* **2003**, *2*, 272 – 277.
[28] G. Decher, *Science* **1997**, *277*, 1232 – 1237.
[29] W. Fischer, S. Markwitz, H. Labischinski, *Eur. J. Biochem.* **1997**, *244*, 913 – 917.
[30] R. J. Doyle, M. L. McDannel, J. R. Helman, U. N. Streips, *J. Bacteriol.* **1975**, *122*, 152 – 158.
[31] M. Virta, S. Lineri, P. Kankaanpaa, M. Karp, K. Peltonen, J. Nuutila, E. M. Lilius, *Appl. Environ. Microbiol.* **1998**, *64*, 515 – 519.
[32] E. Traversa, *Sens. Actuators B* **1995**, *23*, 135 – 156.
[33] S. O. Kasap, *Principals of Electrical Engineering Materials and Devices*, McGraw-Hill, New York **1997**, pp. 284 – 287.

